Modeling the concentration dependence of diffusion in zeolites. I. Analytical theory for benzene in Na-Y

Chandra Saravanan
Department of Chemistry, University of Massachusetts, Amherst, Massachusetts 01003

Scott M. Auerbach[a]
Departments of Chemistry and Chemical Engineering, University of Massachusetts, Amherst, Massachusetts 01003

(Received 12 June 1997; accepted 14 August 1997)

We have developed an analytical expression for the diffusion coefficient of benzene in Na-Y at finite loadings in terms of fundamental rate coefficients. Our theory assumes that benzene molecules jump among S_{II} and W sites, located near Na^+ ions in 6-rings and in 12-ring windows, respectively. We assume that instantaneous occupancies in different supercages are identical, a mean field approximation yielding $D_\theta = \frac{1}{6} k_\theta a_\theta^2$ where $a_\theta \cong 11$ Å is the mean intercage jump length and $1/k_\theta$ is the mean supercage residence time. We show that $k_\theta = \kappa \cdot k_1 \cdot P_1$, where P_1 is the probability of occupying a W site, k_1 is the total rate of leaving a W site, and κ is the transmission coefficient for cage-to-cage motion. We assume $\kappa = \frac{1}{2}$ for all loadings, and derive analytical formulas for the T and θ dependencies of k_1 and P_1, assuming that S_{II} and W site occupancies are either 0 or 1 and that benzenes do not otherwise interact. Exact expressions for P_1 in the canonical and grand canonical ensembles are related for finite systems with a new correspondence rule. For $\theta < 2/3$, the $S_{II} \rightarrow W \rightarrow S_{II}$ process contributes no loading dependence to k_θ, while the $S_{II} \rightarrow W \rightarrow W$ process gives an increasing loading dependence of $1/(2-3\theta)$. For $\theta > \frac{2}{3}$, k_θ initially increases due to enhanced W population, then decreases due to blocking of target W sites. In the article that follows this one we show that our theory agrees quantitatively with simulation, and agrees qualitatively with experiment for low to moderate loadings. © *1997 American Institute of Physics.* [S0021-9606(97)51443-7]

I. INTRODUCTION

The transport properties of adsorbed molecules[1,2] play a central role in catalytic and separation processes[3] that take place within zeolite cavities.[4] Although significant effort has been devoted to understanding diffusion in the zeolites,[1,2] several basic questions persist: What are the fundamental interactions that control the concentration dependence of diffusion in zeolites? How does the competition between entropy and enthalpy modify diffusion in heavily loaded zeolites? Will blocking stable sorption sites tend to increase or decrease the diffusion coefficient? In the present article and in the following article, we begin to address these issues by modeling the concentration dependence of benzene diffusion in Na-Y zeolite.

Dynamics simulations have made a significant impact in this area during the last 10 years,[5–18] and have been particularly useful in modeling rapid diffusion in siliceous zeolites. While the results from these simulations are often reliable, it may be difficult to determine which aspects of a given model are essential to the simulation results. A complementary approach is the development of simple models amenable to analytical solution.[19–25] Although such an approach may not be as predictive as atomistic simulations, analytical modeling can display the physics essential to a process quite clearly. Thorough understanding often requires the interplay of theory and simulation with experiment. In the present article we develop a simple analytical theory for the concentration dependence of benzene diffusion in Na-Y. In the article that follows, denoted as Paper II, we report the results of kinetic Monte Carlo[7,14,26] simulations of benzene in Na-Y to test the accuracy of the analytical formulas derived below.

Significant effort has been devoted to understanding benzene adsorption and diffusion in Na-X and Na-Y,[5,11,27–31] motivated by persistent discrepancies among different experimental probes of mobility.[1] We have recently reported the results of analysis and simulation that greatly simplify benzene diffusion in Na-Y at infinite dilution by focusing on the dynamics of cage-to-cage motion.[14,25,32–34] At finite loadings, however, benzene diffusion is complicated by blocking of stable sites and by intracage benzene–benzene interactions that modify adsorption and activation energies. Despite these influences, measured diffusion coefficients for aromatics in Na-X and Na-Y exhibit a remarkably gentle concentration dependence for low to moderate loadings.[1,35–39]

In the present article we model benzene in Na-Y at finite loadings by taking site blocking into account, i.e. by assuming that site occupancies are either 0 or 1 and that benzenes do not otherwise interact. This site blocking model gives qualitatively accurate results when binding sites are only moderately perturbed by intracage guest–guest interactions. We will address the importance of these interactions in a forthcoming publication.[40] Comparing results from loading models with and without guest–guest interactions will unambiguously indicate the relative importance of site blocking and guest–guest interactions. The simplicity of the site

---

[a] Author to whom correspondence should be addressed.

blocking model allows us to develop an analytical theory for the concentration dependence of benzene diffusion in Na-Y in terms of fundamental rate coefficients. In Paper II we show that our analytical formulas agree quantitatively with simulation results, and agree qualitatively with experiment for low to moderate loadings.

The remainder of this paper is organized as follows: in Sec. II we discuss the assumptions underlying our model including mean field and site blocking approximations. In Sec. III we formulate the derivation, obtain analytical expressions for the factors required, and discuss the resulting concentration and temperature dependencies of the diffusion coefficient. In Sec. IV we summarize the analytical work, foreshadow the simulation results in Paper II, and speculate on the applicability of our approach for other host–guest systems.

II. GENERAL MODEL

A. Lattice model

We model benzene diffusion in Na-Y by replacing the zeolite framework with a three dimensional lattice of binding sites. Such a lattice model is known to reproduce diffusive behavior accurately when site residence times are much longer than travel times between sites.[7,41] This is indeed the case for benzene diffusion in cation-containing faujasites because of the strong charge–quadrupole interactions between Na(II) ions and benzene,[42] as demonstrated by the two-dimensional exchange NMR experiments of Wilhelm *et al.*[43,44]

In this system benzene has two predominant binding sites.[14,28,33] In the primary site, denoted as S_{II}, benzene is facially coordinated to a supercage 6-ring, 2.70 Å above Na(II). In the secondary site, denoted as W, benzene is centered in the 12-ring window separating adjacent supercages, $\sim$5.3 Å from the S_{II} site. Binding sites at Na(I), Na(I′) and Na(III) are not included in our model because Na(III) is negligibly occupied in Na-Y (Si:Al$=$2.0), and because benzene cannot enter the smaller sodalite cages or hexagonal prisms containing Na(I′) and Na(I) cations, respectively. Figure 1 shows a minimum energy hopping path connecting the S_{II} and W sites.[14] Figure 1 also demonstrates that the Na-Y supercage contains four tetrahedrally arranged Na^+ ions and four tetrahedrally arranged 12-ring windows connecting adjacent supercages. Thus, the lattice of benzene binding sites in Na-Y contains four tetrahedrally arranged S_{II} sites and four tetrahedrally arranged, doubly shared W sites per supercage.

Because of the strong Na–benzene interaction the S_{II} site is much more stable than the W site. Indeed, recently reported docking calculations[14,30] of benzene at the S_{II} and W sites in Na-Y suggest that the S_{II} site is more stable by $\sim 25\ \mathrm{kJ\ mol^{-1}}$, indicating that $K_{eq}(S_{II}\rightarrow W) \ll 1$ for loadings of fewer than four molecules per supercage. Figure 2 shows our recently calculated hopping path energies for the $S_{II}\leftrightarrow W$ jump.[14] For a detailed discussion of these binding sites and hopping paths, please see Refs. 14 and 33.

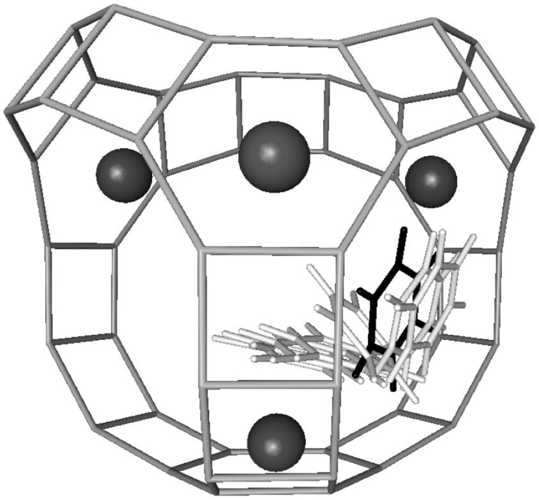

FIG. 1. $S_{II}\leftrightarrow W$ minimum energy path with transition state indicated in bold.

B. Mean field approximation

We can simplify the motion of benzene in Na-Y by imagining that—although hops really take place among S_{II} and W sites—long range motion involves jumps from one ‘‘cage site’’ to an adjacent ‘‘cage site.’’ [25,32] As such, all the S_{II} and W site structure within a cage becomes the internal structure of the cage site. A random walk through Na-Y reduces to hopping on the tetrahedral lattice of supercages, shown in Fig. 3. The diffusion coefficient is then determined by cage residence times and cage-to-cage hopping distances. We have previously shown that for diffusion in Na-Y at infinite dilution, $D=\frac{1}{6}ka^2$ where $a \cong 11$ Å is the mean intercage jump length and $1/k$ is mean cage residence time.[25,32] This result is interesting because we obtain the simple-cubic result even though the simple-cubic partitioning of Na-Y is invalid at the cage-to-cage length scale. Furthermore, simulating the diffusion coefficient via k and a rather than from mean square displacements provides an overwhelming computational speedup. This is because calculating k and a only

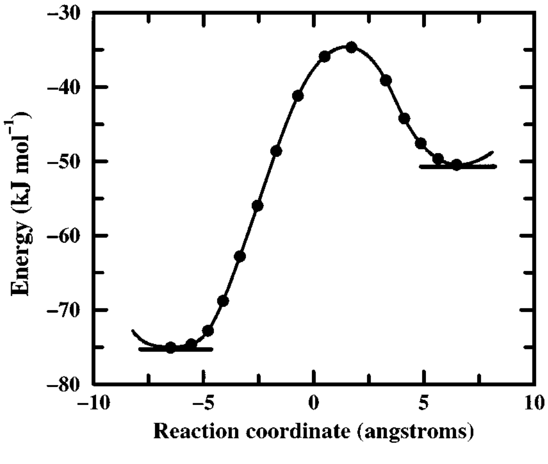

FIG. 2. $S_{II}\leftrightarrow W$ energetics with 41 kJ mol^{-1} activation energy.

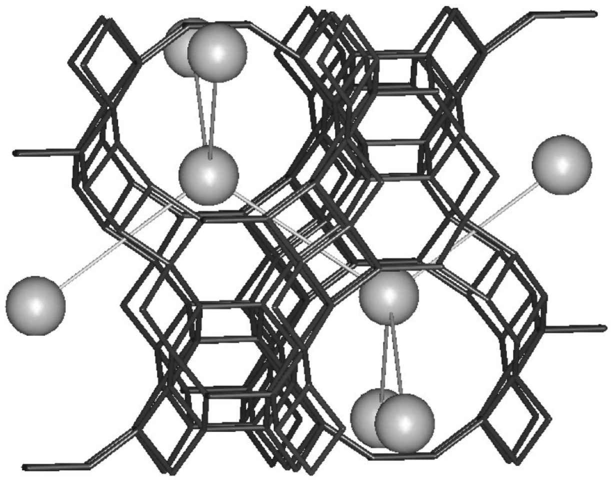

FIG. 3. Tetrahedral connectivity of supercages in the Na-Y unit cell. Balls represent supercage ''sites'' and sticks represent cage-to-cage jumps.

scales as N whereas calculating mean square displacements scales as N^2, where N is the number of Monte Carlo steps.

We can extend this analytical approach to the study of diffusion in Na-Y at finite loadings by making a mean field approximation. To explore this we briefly review how we obtain the infinite dilution diffusion formula, $D=\frac{1}{6}ka^2$. This follows from the Bernoulli distribution for N hops on a tetrahedral lattice,[32] given by:

$$1=1_A 1_B=\sum_{n_{1+},\ldots,n_{4+}}{}' \frac{(N/2)!}{n_{1+}!\cdots n_{4+}!}\, p_{1+}^{n_{1+}}\cdots p_{4+}^{n_{4+}} \cdot \sum_{n_{1-},\ldots,n_{4-}}{}' \frac{(N/2)!}{n_{1-}!\cdots n_{4-}!}\, p_{1-}^{n_{1-}}\cdots p_{4-}^{n_{4-}}, \tag{2.1}$$

where $p_{i+}=p_{i-}=\frac{1}{4}$ for $i=1,\ldots,4$ and the primed summations imply that $\Sigma_{i=1}^{4} n_{i+}=\Sigma_{i=1}^{4} n_{i-}=N/2$. The probability distribution in Eq. (2.1) results because the tetrahedral lattice is composed of two interpenetrating BCC lattices, denoted here as sublattices A and B. During N jumps, $N/2$ jumps visit each sublattice since a random walker must alternate between sublattices at each jump. Each cage in sublattice A has four allowed jumps, labeled by $(1+,2+,3+,4+)$; while each cage in sublattice B has four allowed jumps, labeled by $(1-,2-,3-,4-)$, which are obtained by reversing the A jump directions. The alternation between sublattices causes the Bernoulli distribution for a tetrahedral lattice to separate into an A factor and a B factor as seen in Eq. (2.1). Using this random walk distribution we find that $\langle R^2(N)\rangle=Na^2=kta^2=6Dt$, and hence $D=\frac{1}{6}ka^2$. For more details please see the appendix in Ref. 32.

Equation (2.1) is strictly valid only at infinite dilution where all target cages are empty and hence identical, so that the fundamental cage-to-cage hopping probabilities satisfy $p_{i+}=p_{i-}=\frac{1}{4}$ for $i=1,\ldots,4$. At finite loadings, however, the fundamental jump probabilities depend upon the specific jump process in addition to the instantaneous configuration of random walkers in the starting cage and in adjacent cages. As such there are an enormous number of distinct jump processes to consider at finite loadings. One might envision incorporating configuration dependent fundamental jump probabilities into Eq. (2.1),[15] i.e. $p_{i\pm}\rightarrow p_{i\pm}(\gamma_j,\gamma_k)$, where γ_j and γ_k are the random walker configurations in the starting and target cages, respectively. One might then Boltzmann average over an M-cage configuration space $\boldsymbol{\gamma}\equiv(\gamma_1,\gamma_2,\gamma_3,\ldots,\gamma_M)$ with a lattice gas Hamiltonian,[45] $H(\boldsymbol{\gamma})$, to yield a random walk distribution generalized for finite loadings. Unfortunately this level of sophistication is difficult to treat analytically, although it can be simulated[15] with kinetic Monte Carlo as demonstrated in Paper II.

We can make this problem more analytically tractable with the following mean field approximation: by applying the configurational average directly to each configuration dependent jump probability, we find that

$$\langle p_{i\pm}(\gamma_j,\gamma_k)\rangle=\sum_{\boldsymbol{\gamma}} \frac{e^{-\beta H(\boldsymbol{\gamma})}}{Q(\beta)}\, p_{i\pm}(\gamma_j,\gamma_k)=p_{i\pm}=\tfrac{1}{4}, \tag{2.2}$$

since all cages are identical *on average*. The resulting random walk distribution for finite loadings is identical to that for infinite dilution, and yields $\langle R^2(N)\rangle=Na_\theta^2=k_\theta t a_\theta^2=6D_\theta t$, and hence $D_\theta=\frac{1}{6}k_\theta a_\theta^2$ where θ is the fractional loading, and $1/k_\theta$ and a_θ are the loading dependent mean cage residence time and mean intercage jump length, respectively.

This mean field approximation (MFA) is extremely useful because it serves as the *ansatz* for the analytical theory derived below. The MFA does, however, neglect effects that are occasionally important. The MFA neglects statistical correlation between jumps when, e.g., a random walker jumps into a W site separating nearly empty and full cages. The next jump for that random walker, although uncorrelated from the last jump in the sense of Poisson statistics, is more likely to end up in the nearly empty cage. An extreme manifestation of this effect is a percolation threshold,[46] i.e. a loading above which the diffusion coefficient precipitously decreases. Percolation effects may be important at very high loadings through hysteresis,[47] or for binary or higher mixtures with very different mobilities.[15] Furthermore, the MFA ignores anomalous diffusion, e.g. single file diffusion in one dimensional channel zeolites,[48–50] since the mean square displacement turns out to be linear in time.

Despite these issues, the MFA is likely to be qualitatively accurate when normal diffusion holds. Moreover, the MFA conveniently allows an analytical treatment of the concentration dependence of diffusion in zeolites, which serves as an important complement to simulation. We note that the expression $D_\theta=\frac{1}{6}k_\theta a^2$ is sometimes assumed[1] to be exact. We will address the accuracy of this mean field approximation in a forthcoming publication.[51]

C. Review of infinite dilution

In a previous study[25] we obtained an exact, analytical formula for the cage-to-cage rate coefficient, k, at infinite dilution in terms of fundamental hopping rate coefficients. We review this derivation because it provides the framework for the finite loading diffusion theory derived in Sec. III. In what follows the W and S_{II} sites are denoted sites 1 and 2, respectively.

We imagine a trajectory executed by a single benzene molecule through Na-Y, hopping among S_{II} and W sites. In the limit of a *very* long trajectory, mean residence times at S_{II} and W sites can be used to calculate hopping rate coefficients and equilibrium coefficients in accord with the ergodic hypothesis.[52] The mean supercage residence time, $\langle\tau_c\rangle$, is then given by

$$\begin{aligned}\langle\tau_c\rangle &= \frac{T}{N_{cc}} = \frac{1}{N_{cc}}(T_1+T_2)\\ &= \frac{T_1}{N_{cc}}\left(\frac{T_1+T_2}{T_1}\right) \xrightarrow{T\to\infty} \frac{T_1}{N_{cc}}[1+K_{eq}(1\to 2)],\end{aligned} \tag{2.3}$$

where $T=T_1+T_2$ is the total time of the trajectory, T_1 and T_2 are the total residence times at W and S_{II} sites, respectively, and N_{cc} is the number of cage-to-cage jumps during the trajectory. The long time limit in Eq. (2.3) ensures convergence of T_2/T_1 to the equilibrium coefficient $K_{eq}(1\to 2)=2k_{1\to 2}/k_{2\to 1}$, where $k_{1\to 2}$ and $k_{2\to 1}$ are fundamental rate coefficients (cf. Figs. 1 and 2), and the factor of 2 arises because each W site is shared between two adjacent supercages. The long time limit allows T_1 to be expressed as

$$T_1 = N^{\ddagger}\cdot\frac{T_1}{N^{\ddagger}} = N^{\ddagger}\cdot\langle\tau_1\rangle \xrightarrow{T\to\infty} \frac{N^{\ddagger}}{k_1} = \frac{N^{\ddagger}}{6(k_{1\to 1}+k_{1\to 2})}, \tag{2.4}$$

where $N^{\ddagger}$ is the number of visits to W sites, $\langle\tau_1\rangle$ is the mean W site residence time, $k_1=1/\langle\tau_1\rangle$ is the total rate of leaving the W site, $k_{1\to 1}$ is another fundamental rate coefficient, and the factor of 6 counts available target sites in the Na-Y supercage structure. The long trajectory limit allows one further simplification, namely that $N_{cc}=N^{\ddagger}/2$. The factor of $\frac{1}{2}$ accounts for randomizing in the W site which halves the probability to leave the cage.

Putting these results together, we have

$$\langle\tau_c\rangle = 2\cdot\langle\tau_1\rangle\cdot[1+K_{eq}(1\to 2)] = \frac{1+2k_{1\to 2}/k_{2\to 1}}{3(k_{1\to 1}+k_{1\to 2})}, \tag{2.5}$$

which represents an exact, analytical solution of the master equation determining cage-to-cage motion in terms of fundamental hopping rate coefficients. Equations (2.3)–(2.5) serve as the starting point for the concentration dependent diffusion theory derived below.

D. Site blocking model

In order to model the concentration dependence of self diffusion we must incorporate the effect of guest–guest interactions. On a very qualitative level, repulsive guest–guest forces modify sorption by blocking favorable sorption sites. Attractive guest–guest forces modify sorption sites and energies, ultimately giving rise to phenomena such as capillary condensation. It is not obvious, however, how guest–guest forces modify transport properties. Moreover, it is of great fundamental interest to determine the relative importance of attractive and repulsive guest–guest forces in controlling the concentration dependence of diffusion.

We can disentangle these effects by considering two different models; in the present paper we construct a model in which binding site occupancies are either 0 or 1, and where fundamental hopping rate coefficients calculated at infinite dilution are used.[14] This site blocking model (SBM) will demonstrate how blocking S_{II} and W sites influences diffusion in Na-Y, while ignoring medium to long range interactions. We will address the importance of these interactions in a forthcoming publication.[40] The SBM is motivated by the fact that benzene binding sites in Na-Y are only moderately perturbed by benzene–benzene interactions, as demonstrated by the optimized geometries shown in Fig. 4 using the Na-Y–benzene potential in Ref. 14 and the benzene–benzene potential in Ref. 53. Window site geometries are likewise only moderately perturbed by benzene–benzene interactions. It seems plausible then that simple site blocking should play an important role in determining the concentration dependence of benzene diffusion in Na-Y. The SBM is particularly convenient because its simplicity allows the development of a fully analytical diffusion theory.

In the present study, as in former ones,[14,25,32–34] we estimate rate coefficients at infinite dilution using the Arrhenius formula, in which $k\cong\nu e^{-\beta E_a}$ where ν and E_a are temperature independent. We assume that the Arrhenius prefactors $\{\nu\}$ resemble typical vibrational frequencies, of order 10^{13} s^{-1}. We believe these rate coefficients are sufficiently accurate for the purpose of drawing qualitative conclusions. The calculated hopping activation energies and hypothetical Arrhenius prefactors reported in Ref. 14 are summarized in Table I.

III. ANALYTICAL THEORY FOR FINITE LOADINGS

A. General formulation

In Sec. II we found that $D_\theta=\frac{1}{6}k_\theta a_\theta^2$ within the mean field approximation (MFA). The mean intercage jump length, $a_\theta\cong 11$ Å, depends very weakly upon temperature[32] and loading since this quantity is largely determined by the Na-Y framework structure. We thus focus our attention on the concentration dependence of the mean cage residence time, $\langle\tau_c\rangle=1/k_\theta$. The theory for $\langle\tau_c\rangle$ is obtained by recasting Eqs. (2.3)–(2.5) in language appropriate for finite loadings. Since our ultimate goal is comparing an analytical formula for $\langle\tau_c\rangle$ with canonical kinetic Monte Carlo simulations, our theory for $\langle\tau_c\rangle$ begins by fixing $N=$number of guest molecules, V

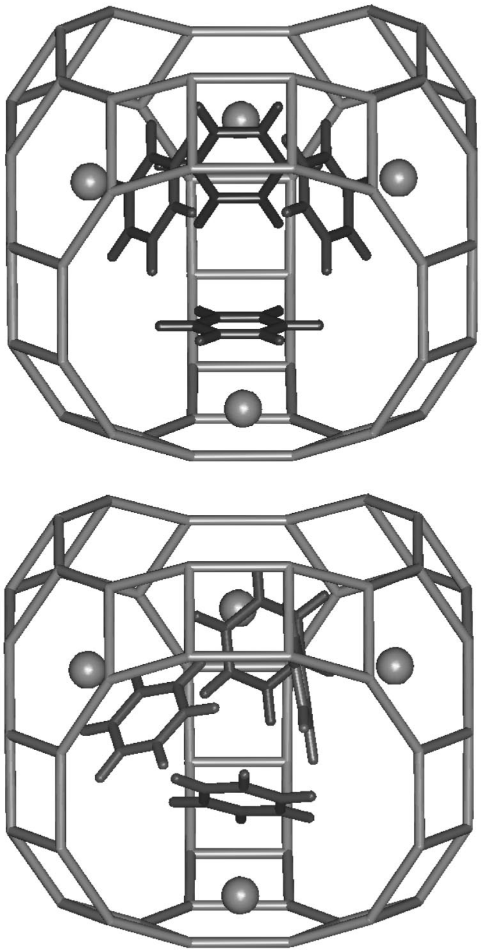

FIG. 4. Optimized benzene binding geometries in Na-Y without (above) and with (below) the influence of benzene–benzene interactions.

TABLE I. Hopping activation energies and hypothetical Arrhenius prefactors for benzene in Na-Y. Our model predicts that leaving the W site is relatively facile.

Jump	Activation energy (kJ mol^{-1})	Arrhenius prefactor (s^{-1})
$S_{II}\to S_{II}$	35	10^{13}
$S_{II}\to W$	41	10^{13}
$W\to S_{II}$	16	10^{13}
$W\to W$	18	10^{13}

=volume of Na-Y which in turn controls the number of available S_{II} and W sites, and $T=(k_B\beta)^{-1}$=absolute temperature of the system. For a given zeolite volume V there are N_1 W sites and N_2 S_{II} sites. For convenience we choose the volume of Na-Y to consist of $\mathscr{V}$ unit cells, each containing 8 supercages and thus 16 W sites and 32 S_{II} sites, so that $N_1=16\mathscr{V}$ and $N_2=32\mathscr{V}$.

We now imagine a trajectory executed by a single benzene molecule through Na-Y loaded with other benzenes, all hopping among S_{II} and W sites. The mean cage residence time is given by:

$$\langle \tau_c \rangle = \frac{T_1}{N_{cc}}\left(\frac{T_1+T_2}{T_1}\right) \xrightarrow{T\to\infty} \frac{N^{\ddagger}\cdot\langle \tau_1\rangle}{N_{cc}}[1+K_{eq}(1\to 2)], \tag{3.1}$$

where all the quantities in Eq. (3.1) are defined as in Eqs. (2.3)–(2.5). We now define the transmission coefficient according to $\kappa\equiv N_{cc}/N^{\ddagger}$. The transmission coefficient is the probability of cage-to-cage motion for a benzene already occupying a W site. At infinite dilution $\kappa=\frac{1}{2}$. With this quantity the mean cage residence time becomes:

$$\langle \tau_c \rangle = \frac{\langle \tau_1\rangle}{\kappa}[1+K_{eq}(1\to 2)]. \tag{3.2}$$

The benefit of defining κ should now be clear: $N^{\ddagger}$ and N_{cc} are eliminated in favor of κ, a quantity about which we have insight. The cage-to-cage rate coefficient is thus given by:

$$k_{\theta}=\kappa\cdot k_1\cdot\frac{1}{[1+K_{eq}(1\to 2)]}=\kappa\cdot k_1\cdot\left(\frac{T_1}{T_1+T_2}\right)=\kappa\cdot k_1\cdot P_1. \tag{3.3}$$

Equation (3.3) has the following pedagogically attractive interpretation. The rate of cage-to-cage motion is a product of three concentration dependent factors: P_1 is the probability of occupying a W site, k_1 is the total rate of leaving a W site, and κ is the probability of cage-to-cage motion when starting from a W site. Note that setting $\kappa=\frac{1}{2}$, $K_{eq}(1\to 2)=2k_{1\to 2}/k_{2\to 1}$, and $k_1=6(k_{1\to 1}+k_{1\to 2})$ gives the infinite dilution limit in Eq. (2.5). Below we pursue analytical expressions for the concentration dependencies of these three quantities.

B. Transmission coefficient

The transmission coefficient is a measure of the extent to which jumps involving W sites are statistically correlated. As discussed in Sec. IIB, a random walker that jumps into a W site separating nearly empty and full cages is more likely to end up in the nearly empty cage. Unfortunately the statistical correlation determining the transmission coefficient is difficult to treat analytically, although it can be simulated with kinetic Monte Carlo[7,26] as demonstrated in Paper II. Indeed, the *ansatz* of this article is a MFA exploiting the fact that cages are identical on average. To be consistent with our previous MFA, we make a MFA for the tranmission coefficient yielding $\kappa=\frac{1}{2}$ for all loadings. In Paper II we will see that the transmission coefficient simulated at $T=300$ K is close to $\frac{1}{2}$ for low to moderate loadings, and falls to $\sim\frac{3}{8}$ at nearly full loading.

C. Equilibrium coefficient

We now derive an approximate analytical formula for the concentration dependence of $P_1=[1+K_{eq}(1\to 2)]^{-1}$ keeping N, V and T fixed. The simplicity of the site blocking model allows us, in addition, to derive exact expressions for $K_{eq}(1\to 2)$ for verifying the accuracy of the approximate formula. While it is straightforward to formulate an exact canonical expression for $K_{eq}(1\to 2)$, it is not trivial to evaluate the expression for arbitrarily large volumes. This is important for quantifying finite size effects in both our theory and simulation results. As discussed in the next section, it is much more straightforward to calculate $K_{\mathrm{eq}}(1\rightarrow 2)$ using the grand canonical ensemble, keeping μ, V and T fixed. However, since our ultimate goal is comparison with canonical kinetic Monte Carlo simulations for finite systems, we need to determine a correspondence between grand canonical averages and canonical averages *away from* the thermodynamic limit, i.e. away from the limit $V\rightarrow\infty$. In the next three sections we develop for $K_{\mathrm{eq}}(1\rightarrow 2)$: exact canonical and grand canonical expressions, an approximate canonical formula, and the correspondence between grand canonical and canonical results for finite volumes.

1. Exact expression

a. Canonical ensemble: The equilibrium coefficient is given by $K_{\mathrm{eq}}(1\rightarrow 2)=\langle n_2\rangle/\langle n_1\rangle$, where n_1 and n_2 are the fluctuating numbers of molecules at W and $\mathrm{S_{II}}$ sites, respectively. In the canonical ensemble $N=\langle n_1\rangle+\langle n_2\rangle$, so that $K_{\mathrm{eq}}(1\rightarrow 2)=(N-\langle n_1\rangle)/\langle n_1\rangle$, where $\langle n_1\rangle$ is given by:

$$\langle n_1\rangle=\sum_{n_1=n_1^{\min}}^{n_1^{\max}} P(n_1)\cdot n_1, \tag{3.4}$$

and the summation limits are $n_1^{\min}=\max(0,N-N_2)$ and $n_1^{\max}=\min(N,N_1)$. The upper limit results because the number of molecules at W sites cannot be greater than the total number of molecules or the number of W sites. The lower limit results because the number of molecules at W sites cannot be smaller than the total number of molecules minus the number of $\mathrm{S_{II}}$ sites, i.e. $N-N_2$, when $N-N_2>0$. The probability in Eq. (3.4) is given by:

$$P(n_1)=\frac{\Omega(n_1)e^{-\beta[n_1E_1+(N-n_1)E_2]}}{Q(N,V,\beta)}, \tag{3.5}$$

where E_1 and E_2 are the site binding energies at W and $\mathrm{S_{II}}$ sites, respectively, and the microcanonical prefactor is given by:

$$\begin{aligned}\Omega(n_1)&=\binom{N_1}{n_1}\binom{N_2}{N-n_1}\\&=\frac{N_1!}{n_1!(N_1-n_1)!}\cdot\frac{N_2!}{(N-n_1)!(N_2-N+n_1)!}.\end{aligned} \tag{3.6}$$

In Eq. (3.5), $Q(N,V,\beta)$ is the canonical partition function given by:

$$Q(N,V,\beta)=\sum_{n_1=n_1^{\min}}^{n_1^{\max}}\Omega(n_1)e^{-\beta[n_1E_1+(N-n_1)E_2]}. \tag{3.7}$$

Evaluating $K_{\mathrm{eq}}(1\rightarrow 2)$ analytically using Eqs. (3.4)–(3.7) is difficult because fixing N couples the combinatorial coefficients. Although we can evaluate $K_{\mathrm{eq}}(1\rightarrow 2)$ numerically for $\mathscr{V}=1$ and 8 as shown below, the calculation becomes cumbersome for larger volumes because of the combinatorial coefficients required.

b. Grand canonical ensemble: We solve this problem by calculating $K_{\mathrm{eq}}(1\rightarrow 2)$ in the grand canonical ensemble, fixing μ, V and T. As mentioned above, we must be careful when comparing averages from grand canonical and canonical calculations for small systems; this issue is addressed below. The grand canonical partition function is given by:

$$\begin{aligned}\Xi(\mu,V,\beta)&=\sum_{N=0}^{N_{\max}}Q(N,V,\beta)e^{\beta\mu N}\\&=\sum_{N=0}^{N_1+N_2}\sum_{n_1=n_1^{\min}}^{n_1^{\max}}\binom{N_1}{n_1}\binom{N_2}{N-n_1}p_1^{n_1}p_2^{N-n_1}e^{\beta\mu N},\end{aligned} \tag{3.8}$$

where $p_i=e^{-\beta E_i}$ for $i=1$ and 2. Allowing N to fluctuate gives a second summation in the partition function. The double sum can be expressed in terms of (n_1,n_2) instead of (N,n_1) where $n_2=N-n_1$, thereby decoupling the partition function according to:

$$\begin{aligned}\Xi(\mu,V,\beta)&=\sum_{n_1=0}^{N_1}\sum_{n_2=0}^{N_2}\binom{N_1}{n_1}\binom{N_2}{n_2}p_1^{n_1}p_2^{n_2}e^{\beta\mu(n_1+n_2)}\\&=(1+p_1e^{\beta\mu})^{N_1}\cdot(1+p_2e^{\beta\mu})^{N_2},\end{aligned} \tag{3.9}$$

where Eq. (3.9) results from the binomial theorem.[54] The average loading $\langle N\rangle_\mu$ is obtained with the standard thermodynamic derivative:[45]

$$\begin{aligned}\langle N\rangle_\mu&=\left[\frac{\partial\ln\Xi}{\partial(\beta\mu)}\right]_{V,\beta}=\frac{N_1}{1+e^{\beta(E_1-\mu)}}+\frac{N_2}{1+e^{\beta(E_2-\mu)}}\\&=\langle n_1\rangle_\mu+\langle n_2\rangle_\mu.\end{aligned} \tag{3.10}$$

Equation (3.10) is formally identical to that obtained for an ideal gas of N_1 fermions with energy E_1 and N_2 fermions with energy E_2. This analogy arises because $\mathrm{S_{II}}$ and W sites can have occupancies of 0 or 1 as in Fermi-Dirac statistics.[45] Based on Eq. (3.10) the grand canonical equilibrium coefficient is given by:

$$K_{\mathrm{eq}}(1\rightarrow 2)=\frac{N_2}{N_1}\cdot\frac{1+e^{\beta(E_1-\mu)}}{1+e^{\beta(E_2-\mu)}}=2\cdot\frac{1+e^{\beta(E_1-\mu)}}{1+e^{\beta(E_2-\mu)}}. \tag{3.11}$$

Equation (3.11) shows that the grand canonical equilibrium coefficient within the site blocking model formally depends upon μ and β, but not on V. The results in Eqs. (3.10) and (3.11) can be related to the canonical ensemble by inverting $\langle N\rangle_\mu$ as a function of μ, then evaluating $K_{\mathrm{eq}}(1\rightarrow 2)$ as a function of $\mu(N)$. This inversion is itself difficult to perform analytically, rendering Eqs. (3.10) and (3.11) a convenient numerical approach for determining how the exact grand canonical equilibrium coefficient varies with loading.

Before deriving the approximate canonical formula in the next section, it is instructive to consider various limits of the exact canonical and grand canonical equilibrium coefficients. It is straightforward to show that for any volume V, the canonical equilibrium coefficient satisfies $K_{\mathrm{eq}}(1\rightarrow 2)=2e^{-\beta(E_2-E_1)}$ for $N=1$, and $K_{\mathrm{eq}}(1\rightarrow 2)=2$ for $N=N_1+N_2$. Likewise for any volume V, the grand canonical equilibrium coefficient satisfies $K_{\mathrm{eq}}(1\rightarrow 2)=2e^{-\beta(E_2-E_1)}$ for

$\mu\to-\infty$, and $K_{\mathrm{eq}}(1\to 2)=2$ for $\mu\to\infty$. Although the full loading limits correspond between the two ensembles, i.e. $\lim_{\mu\to\infty}\langle N\rangle_\mu = N_1+N_2$, the infinite dilution limits do not correspond because $\lim_{\mu\to-\infty}\langle N\rangle_\mu=0$, while infinite dilution for the canonical ensemble means $N=1$. Thus one has to be careful in associating N from the canonical ensemble with $\langle N\rangle_\mu$ from the grand canonical ensemble. Although the correspondence becomes straightforward when comparing fractional loadings for infinite systems, i.e. $\theta\equiv N/(N_1+N_2)$ when $N_1+N_2\to\infty$, we require a correspondence between these grand canonical results and canonical simulations of finite systems; such a rule is developed below.

2. Leading order approximation

In the previous section we developed exact expressions for the equilibrium coefficient in various ensembles. We would prefer, however, to have an analytical expression for $K_{\mathrm{eq}}(1\to 2)$ showing explicit dependencies on N and T. In this section we obtain such a formula using a leading order approximation in the canonical ensemble. We exploit the fact that at relevant temperatures the $\mathrm{S_{II}}$ site is much more stable than the W site, i.e. $\beta(E_1-E_2)\gg 1$, to obtain a simple formula for $K_{\mathrm{eq}}(1\to 2)$. We first order the summation in Eq. (3.4) in powers of the small parameter $\varepsilon\equiv e^{-\beta(E_1-E_2)}$. The canonical equilibrium coefficient, $K_{\mathrm{eq}}(1\to 2)=(N-\langle n_1\rangle)/\langle n_1\rangle$, takes the form:

$$K_{\mathrm{eq}}(1\to 2)=\sum_{n_1=n_1^{\min}}^{n_1^{\max}}\Omega(n_1)\varepsilon^{n_1}\times(N-n_1)\Bigg/\sum_{n_1'=n_1^{\min}}^{n_1^{\max}}\Omega(n_1')\varepsilon^{n_1'}n_1'. \tag{3.12}$$

In order to extract an analytical formula from this expression, we need to specify N to make the summation limits concrete. Since $\varepsilon\ll 1$ the summand decays rapidly, obviating the need to specify the upper limit. There are thus two cases to consider: $N\leq N_2$ for which $n_1^{\min}=0$, and $N>N_2$ for which $n_1^{\min}=N-N_2$.

a. Case 1: $N\leq N_2$: By dividing numerator and denominator in Eq. (3.12) by the first term in the numerator, the equilibrium coefficient for $N\leq N_2$ becomes:

$$K_{\mathrm{eq}}(1\to 2)=\frac{1+\dfrac{N-1}{N}\dfrac{\Omega(1)}{\Omega(0)}\varepsilon+\dfrac{N-2}{N}\dfrac{\Omega(2)}{\Omega(0)}\varepsilon^2+\cdots}{0+\dfrac{1}{N}\dfrac{\Omega(1)}{\Omega(0)}\varepsilon+\dfrac{2}{N}\dfrac{\Omega(2)}{\Omega(0)}\varepsilon^2+\cdots}=\frac{1+\dfrac{N_1(N-1)}{N_2-N+1}\varepsilon+\dfrac{N_1(N_1-1)(N-1)(N-2)}{2(N_2-N+1)(N_2-N+2)}\varepsilon^2+\cdots}{0+\dfrac{N_1}{N_2-N+1}\varepsilon+\dfrac{N_1(N_1-1)(N-1)}{(N_2-N+1)(N_2-N+2)}\varepsilon^2+\cdots}. \tag{3.13}$$

If we consider only the first nonzero term in numerator and denominator, an approximation whose validity we discuss below, the equilibrium coefficient becomes:

$$K_{\mathrm{eq}}(1\to 2)\cong\frac{N_2-N+1}{N_1\varepsilon}=\frac{N_2-N+1}{N_1}e^{-\beta(E_2-E_1)}. \tag{3.14}$$

Equation (3.14) provides an analytical expression for $K_{\mathrm{eq}}(1\to 2)$ showing explicit dependencies on N and T. Note that the concentration dependence in Eq. (3.14) gives the correct infinite dilution limit. Equation (3.14) is exactly the equilibrium coefficient for a single molecule in Na-Y with $N-1$ blocked $\mathrm{S_{II}}$ sites. This is consistent with the leading order approximation, which considers only single excitations to W sites. The equilibrium coefficient decreases with loading, i.e. becomes less favorable for occupying $\mathrm{S_{II}}$ sites, because of the decreasing $\mathrm{S_{II}}$ configurational entropy associated with blocking $N-1$ $\mathrm{S_{II}}$ sites.

We can obtain a simple estimate for when we expect Eq. (3.14) to be accurate. Considering the lowest order terms in ε that are ignored relative to the terms that are taken, the leading order approximation is valid when:

$$x_1\equiv\frac{N_1N}{N_2-N+1}e^{-\beta(E_1-E_2)}\ll 1. \tag{3.15}$$

Equation (3.15) shows that increasing N, V or T will make Eq. (3.14) less accurate. Assuming $\mathscr{V}=1$, $N=16$ and adopting the somewhat arbitrary accuracy criterion that $x_1\leq 0.1$, the leading order approximation is valid for $T\leq 600$ K. Assuming $T=300$ K, $N=16$ and $x_1\leq 0.1$, the leading order approximation is valid for $\mathscr{V}\leq 140$ unit cells.

b. Case 2: $N>N_2$: Using the same approach as before, but now with the lower limit $n_1^{\min}=N-N_2$, the equilibrium coefficient for $N>N_2$ becomes:

$$\begin{aligned}K_{\mathrm{eq}}(1\to 2)&=\frac{1+\dfrac{N_2-1}{N_2}\dfrac{\Omega(N-N_2+1)}{\Omega(N-N_2)}\varepsilon+\cdots}{\dfrac{N-N_2}{N_2}+\dfrac{N-N_2+1}{N_2}\dfrac{\Omega(N-N_2+1)}{\Omega(N-N_2)}\varepsilon+\cdots}\\&=\frac{1+\dfrac{(N_2-1)(N_1+N_2-N)}{N-N_2+1}\varepsilon+\cdots}{\dfrac{N-N_2}{N_2}+(N_1+N_2-N)\varepsilon+\cdots}.\end{aligned} \tag{3.16}$$

Ignoring all but the lowest order terms in ε, the high loading equilibrium coefficient becomes:

$$K_{\mathrm{eq}}(1\to 2)\cong\frac{N_2}{N-N_2}. \tag{3.17}$$

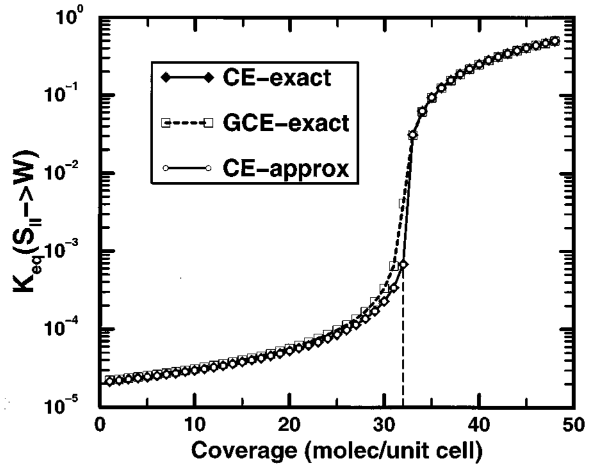

FIG. 5. $K_{\mathrm{eq}}(2\rightarrow 1)$ for $\mathscr{V}=1$ and $T=300$ K using exact canonical, exact grand canonical and leading order canonical methods. Approximate and exact canonical agree perfectly, while exact canonical and grand canonical do not.

Equation (3.17) predicts that $K_{\mathrm{eq}}(1\rightarrow 2)$ is independent of T for $N>N_2$. Note that the concentration dependence in Eq. (3.17) gives the correct full loading limit. Equation (3.17) is exactly the equilibrium coefficient for N_2 occupied S_{II} sites and $N-N_2$ occupied W sites. The equilibrium coefficient decreases with loading, i.e. becomes more favorable for occupying W sites, because each new sorbed molecule is forced to occupy a W site. Equation (3.17) is valid when:

$$x_2 \equiv \frac{N_2(N_1+N_2-N)}{N-N_2+1} e^{-\beta(E_1-E_2)} \ll 1. \tag{3.18}$$

Equation (3.18) shows that decreasing N, increasing T or increasing V will make Eq. (3.17) less accurate. Assuming $\mathscr{V}=1$, $N=40$ and $x_2 \leqslant 0.1$, the leading order approximation is valid for $T \leqslant 525$ K. Assuming $T=300$ K, $N=40$ and $x_2 \leqslant 0.1$, the leading order approximation is valid for $\mathscr{V} \leqslant 75$ unit cells.

We have thus found that Eqs. (3.14) and (3.17) are most accurate for sufficiently low T and V, and for loadings $N \approx N_2$. In Paper II we will use Eqs. (3.14) and (3.17) to interpret kinetic Monte Carlo results for $\mathscr{V}=1$ and $T=300$ K. Figure 5 shows $K_{\mathrm{eq}}(2\rightarrow 1)=1/K_{\mathrm{eq}}(1\rightarrow 2)$, a quantity that will soon become important, calculated as a function of loading for $\mathscr{V}=1$ and $T=300$ K using the exact canonical, exact grand canonical and leading order canonical methods. Figure 5 shows that while our analytical approximation gives essentially perfect agreement with the exact canonical results, the exact canonical and grand canonical values do *not* agree perfectly; we resolve this discrepancy below. Since our analytical formulas are accurate for low enough temperatures, they serve as a useful complement to simulation methods which sample efficiently at high temperatures. In the next section we will show that Eqs. (3.14) and (3.17) turn out to be accurate for any volume V as long as $N \not\approx N_2$.

3. Canonical and grand canonical averages

In the previous sections we developed numerical and analytical approaches for determining the concentration dependence of $K_{\mathrm{eq}}(1\rightarrow 2)$ for use in Eq. (3.3). We found that the grand canonical ensemble provides a convenient, numerically exact approach for calculating $K_{\mathrm{eq}}(1\rightarrow 2)$ for any volume V. In addition, the canonical ensemble gives simple analytical formulas for $K_{\mathrm{eq}}(1\rightarrow 2)$ which are valid for a significant range of T and V. It turns out that Eqs. (3.14) and (3.17) are valid for any V as long as T is not too high and $N \not\approx N_2$. We would like to use the grand canonical results to confirm the accuracy of the canonical formulas for arbitrary volumes. Statistical mechanics dictates that averages from these ensembles will agree in the thermodynamic limit,[55] i.e. for a given fractional loading θ as $V\rightarrow\infty$, but not necessarily for finite systems. In this section we develop a simple correspondence rule for comparing averages from these ensembles for any V.

Recall from Eqs. (3.4)–(3.11) the correspondence at infinite dilution $N=1 \Leftrightarrow \lim_{\mu\rightarrow-\infty}\langle N\rangle_\mu=0$, and at full loading $N=N_1+N_2 \Leftrightarrow \lim_{\mu\rightarrow\infty}\langle N\rangle_\mu=N_1+N_2$. A rule consistent with these boundary conditions can be extracted from our leading order formulas taken to the thermodynamic limit for a given fractional loading:

$$\frac{N_2-N+1}{N_1\varepsilon} \xrightarrow{V\rightarrow\infty} \frac{N_2-N}{N_1\varepsilon} \Leftrightarrow \frac{N_2-\langle N\rangle_\mu}{N_1\varepsilon}, \quad \text{for } N \leqslant N_2, \tag{3.19}$$

$$\frac{N_2}{N-N_2} \xrightarrow{V\rightarrow\infty} \frac{N_2}{N-N_2} \Leftrightarrow \frac{N_2}{\langle N\rangle_\mu - N_2}, \quad \text{for } N>N_2. \tag{3.20}$$

Equations (3.19) and (3.20) suggests at finite V the correspondence:

$$\langle N\rangle_\mu = N-1, \quad \text{for } N \leqslant N_2, \tag{3.21}$$

$$\langle N\rangle_\mu = N, \quad \text{for } N>N_2. \tag{3.22}$$

For any N, V and T, Eqs. (3.21) and (3.22) indicate how to calculate $\mu(N,V,T)$. The exact canonical equilibrium coefficient is obtained by substituting $\mu(N,V,T)$ into Eq. (3.11). Equations (3.21) and (3.22) are consistent with the boundary conditions noted above and give fractional loadings that agree in the thermodynamic limit. Moreover, the fractional loadings for $N \leqslant N_2$ differ by $\mathscr{O}(1/V)$ in agreement with formal statistical mechanics.[55] It is interesting that $\langle N\rangle_\mu = N$ for high loadings. This is plausible because at such loadings the overwhelming majority of configurations involve occupancies only at W sites. The system thus mimics a simple lattice with a single site energy, E_1. For such a lattice the canonical and grand canonical ensembles sample identical fluctuations since $E=n_1E_1$, i.e. fluctuations in energy E and number n_1 are the same.

Figure 6 shows the percent difference between the grand canonical $K_{\mathrm{eq}}(2\rightarrow 1)$ and the exact canonical value for $T=300$ K, $\mathscr{V}=1$ and 8. The grand canonical and canonical values agree more closely for larger volume, and agree almost perfectly when applying the shift rule $\langle N\rangle_\mu = N-1$ for

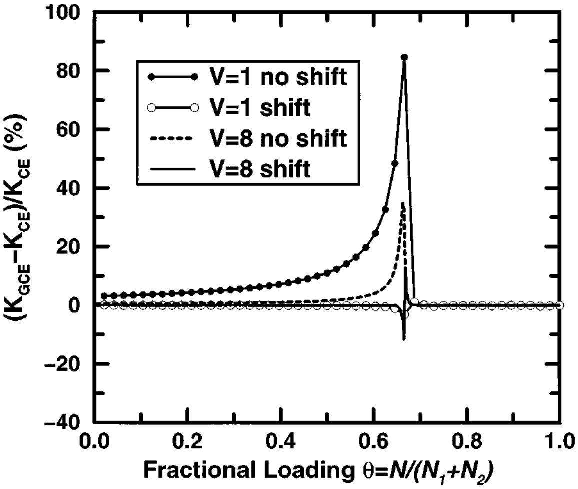

FIG. 6. Percent difference of grand canonical $K_{\mathrm{eq}}(2\rightarrow1)$ from exact canonical value for $T=300$ K, $\mathscr{V}=1$ and 8. Grand canonical and canonical values agree more closely for larger volume, and agree almost perfectly when applying the shift rule $\langle N\rangle_\mu=N-1$ for $N\leqslant N_2$. The glitch at $N=N_2$ is numerical error in the exact canonical calculation.

$N\leqslant N_2$. The glitch at $N=N_2$ is numerical error in the exact canonical calculation, which grows with volume. Figure 6 demonstrates that we can use grand canonical results to confirm the accuracy of the analytical formulas for any volume, as long as we apply the shift rule. Figure 7 compares our analytical formulas for $K_{\mathrm{eq}}(2\rightarrow1)$ with the shifted grand canonical result for $T=300$ K and $\mathscr{V}=1500$, a system with accuracy parameters $x_1\cong1.1$ from Eq. (3.15) and $x_2\cong2.0$ from Eq. (3.18). Even though the analytical formulas are being applied outside their proper regimes, Fig. 7 indicates that the formulas capture the behavior of $K_{\mathrm{eq}}(2\rightarrow1)$ quite accurately away from the fractional loading $\theta=\frac{2}{3}$. We thus regard our analytical estimates of $K_{\mathrm{eq}}(2\rightarrow1)$ rather useful for determining the concentration dependence of the window population, P_1, in Eq. (3.3).

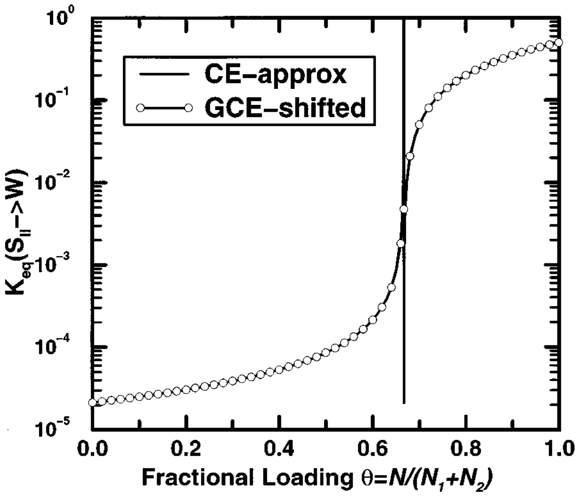

FIG. 7. Comparison of analytical formulas and shifted grand canonical values for $K_{\mathrm{eq}}(2\rightarrow1)$ at $T=300$ K and $\mathscr{V}=1500$, a system outside the accuracy regimes of the analytical formulas. Excellent agreement is obtained away from $\theta=\frac{2}{3}$.

D. Window residence time

We now derive approximate analytical formulas for the concentration dependence of $\langle\tau_1\rangle$, the mean W site residence time, keeping N, V and T fixed. At infinite dilution, the average in $\langle\tau_1\rangle$ is over random jump times taken from a Poisson distribution, $P(t)=k_1e^{-k_1t}$, where $k_1=6(k_{1\rightarrow1}+k_{1\rightarrow2})=1/\langle\tau_1\rangle$ is the total rate coefficient for jumping away from a W site. At finite loadings the calculation of $\langle\tau_1\rangle$ for a given molecule involves, in addition, an average over random walker configurations $\boldsymbol{\gamma}$, as in Eq. (2.2). Since a random walker cannot jump to an occupied site, the total rate coefficient for a molecule to leave a site depends upon the occupancy of potential target sites, i.e. nearest neighbor sites. The mean W site residence time can be expressed as:

$$\langle\tau_1\rangle=\left\langle\frac{1}{k_1(\boldsymbol{\gamma})}\right\rangle'=\left\langle\frac{1}{(6-\tilde{n}_1)k_{1\rightarrow1}+(6-\tilde{n}_2)k_{1\rightarrow2}}\right\rangle', \tag{3.23}$$

where $\tilde{n}_1,\tilde{n}_2=0,\ldots,6$ are the numbers of occupied nearest neighbor W and S_{II} sites, respectively, and the primed average omits configurations that give $k_1(\boldsymbol{\gamma})=0$. In what follows we obtain analytical formulas for $\langle\tau_1\rangle$ making assumptions consistent with the mean field-leading order approximations discussed above. Since there is no exact formula for $\langle\tau_1\rangle$, we will justify our approach using mathematical and physical arguments. As with the derivation of $K_{\mathrm{eq}}(1\rightarrow2)$, it is useful to consider two loading regimes: $N\leqslant N_2$ and $N>N_2$.

1. Case 1: $N\leqslant N_2$

We begin by assuming that for $N\leqslant N_2$, configurations with more than one occupied W site contribute negligibly to the average in Eq. (3.23). We can thus set $\tilde{n}_1$ to zero and focus on averaging $\tilde{n}_2$. Here it is useful to consider two limiting cases: $\langle\tilde{n}_2\rangle\gtrsim0$ and $\langle\tilde{n}_2\rangle\lesssim6$, corresponding to $N\gtrsim1$ and $N\lesssim N_2$, respectively. In the former case, we express $\langle\tau_1\rangle$ as:

$$\begin{aligned}\langle\tau_1\rangle&=\frac{1}{6(k_{1\rightarrow1}+k_{1\rightarrow2})}\left\langle\frac{1}{1-\alpha_1\tilde{n}_2/6}\right\rangle\\&=\frac{1}{6(k_{1\rightarrow1}+k_{1\rightarrow2})}\left\langle1+\frac{\alpha_1\tilde{n}_2}{6}+\left(\frac{\alpha_1\tilde{n}_2}{6}\right)^2+\cdots\right\rangle,\end{aligned} \tag{3.24}$$

where the prime is omitted because $\tilde{n}_1=0$, and the geometric expansion converges because $\alpha_1=k_{1\rightarrow2}/(k_{1\rightarrow1}+k_{1\rightarrow2})$ and $\tilde{n}_2/6$ are both less than one. When $N=1$, $\tilde{n}_2=0$ for all configurations and the infinite dilution result is obtained. For loadings slightly above $N=1$, we can estimate the concentration dependence of $\langle\tau_1\rangle$ by truncating the geometric expansion in Eq. (3.24) at first order, giving:

$$\begin{aligned}\langle\tau_1\rangle &\cong \frac{1}{6(k_{1\to1}+k_{1\to2})}\left(1+\frac{\alpha_1\langle\tilde{n}_2\rangle}{6}\right)\\ &\cong \frac{1}{6(k_{1\to1}+k_{1\to2})}\left(\frac{1}{1-\alpha_1\langle\tilde{n}_2\rangle/6}\right)\\ &= \frac{1}{6k_{1\to1}+6(1-\langle\tilde{n}_2\rangle/6)k_{1\to2}},\end{aligned} \tag{3.25}$$

where the second approximation in Eq. (3.25) results from resumming the truncated geometric expansion assuming $\langle\tilde{n}_2\rangle/6\ll 1$. We have reduced the problem to determining $\langle\tilde{n}_2\rangle/6$, the probability of occupying nearest neighbor S_{II} sites. Since all S_{II} sites are equivalent in the site blocking model, the probability of occupying nearest neighbor S_{II} sites is equivalent to the probability of occuping S_{II} sites in general, i.e. $\langle\tilde{n}_2\rangle/6=(N-1)/N_2$, where we have assumed that $N-1$ molecules occupy S_{II} sites and one molecule occupies a W site. The total rate coefficient for a molecule to leave a W site for small N is thus

$$k_1=\frac{1}{\langle\tau_1\rangle}=6k_{1\to1}+6\left(1-\frac{N-1}{N_2}\right)k_{1\to2}. \tag{3.26}$$

Equation (3.26) produces the correct infinite dilution limit, and predicts that $\langle\tau_1\rangle$ increases with loading because adding molecules blocks target S_{II} sites.

We now consider the other limiting case for $N\leqslant N_2$, namely that $\langle\tilde{n}_2\rangle\lesssim 6$ corresponding to $N\lesssim N_2$. Using the approach developed in Eqs. (3.24) and (3.25), and defining $\alpha_2\equiv k_{1\to2}/k_{1\to1}$, we obtain:

$$\begin{aligned}\langle\tau_1\rangle &= \frac{1}{6k_{1\to1}}\left\langle\frac{1}{1-\alpha_2(1-\tilde{n}_2/6)}\right\rangle\\ &= \frac{1}{6k_{1\to1}}\left\langle 1+\alpha_2\left(1-\frac{\tilde{n}_2}{6}\right)+\left[\alpha_2\left(1-\frac{\tilde{n}_2}{6}\right)\right]^2+\cdots\right\rangle\\ &\cong \frac{1}{6k_{1\to1}}\left[1+\alpha_2\left(1-\frac{\langle\tilde{n}_2\rangle}{6}\right)\right]\\ &\cong \frac{1}{6k_{1\to1}}\left[\frac{1}{1-\alpha_2(1-\langle\tilde{n}_2\rangle/6)}\right]\\ &= \frac{1}{6k_{1\to1}+6(1-\langle\tilde{n}_2\rangle/6)k_{1\to2}},\end{aligned} \tag{3.27}$$

a final result identical to that in Eq. (3.25). As a result, the total rate coefficient for a molecule to leave a W site for $N\lesssim N_2$ is the same as that for $N\gtrsim 1$ in Eq. (3.26). The fact that identical results are obtained for $N\gtrsim 1$ and $N\lesssim N_2$ is physically plausible for the following reason. When $N\gtrsim 1$ a molecule leaving a W site is likely to have all target S_{II} sites empty. Likewise, when $N\lesssim N_2$ a molecule leaving a W site is likely to have all target S_{II} sites occupied. Thus, in both cases the distribution over $\tilde{n}_2$ values is very narrow, giving $\langle\tilde{n}_2^k\rangle\cong\langle\tilde{n}_2\rangle^k$ for all powers k. The mathematical consequence of this is:

$$\left\langle\frac{1}{1-\alpha\tilde{n}_2}\right\rangle\cong\frac{1}{1-\alpha\langle\tilde{n}_2\rangle}, \tag{3.28}$$

which is precisely the result obtained in Eqs. (3.25) and (3.27). Although the concentration dependence of k_1 in Eq. (3.26) is not expected to be as accurate for $N\approx N_2/2$ as it is for $N\gtrsim 1$ and $N\lesssim N_2$, Eq. (3.26) is a very convenient way to interpolate between these two limits, and is assumed valid for all loadings $N\leqslant N_2$.

2. Case 2: $N>N_2$

To obtain the concentration dependence of k_1 for $N>N_2$ we use the same approach as for $N\leqslant N_2$, except now we assume that $\tilde{n}_2=6$ and $\tilde{n}_1\neq 0$, since all S_{II} sites and some W sites are likely to be occupied. The result is:

$$\langle\tau_1\rangle=\left\langle\frac{1}{(6-\tilde{n}_1)k_{1\to1}}\right\rangle'\cong\frac{1}{(6-\langle\tilde{n}_1\rangle')k_{1\to1}}, \tag{3.29}$$

where we have utilized the general approximation scheme in Eq. (3.28). We have now reduced the problem to determining the probability of occupying nearest neighbor W sites, which is equivalent to the probability of occuping W sites in general, i.e. $\langle\tilde{n}_1\rangle'/6=(N-N_2-1)/(N_1-1)$. Here we assume that one molecule occupies a W site, N_2 molecules occupy S_{II} sites, and $N-N_2-1$ molecules are distributed among the remaining N_1-1 W sites, potentially blocking a jump out of the initial W site. The total rate coefficient for a molecule to leave a W site for $N>N_2$ is thus

$$k_1=\frac{1}{\langle\tau_1\rangle}=6\left(1-\frac{N-N_2-1}{N_1-1}\right)k_{1\to1}. \tag{3.30}$$

Equation (3.30) produces the correct full loading result, i.e. $k_1=0$ for $N=N_1+N_2$, and predicts that $\langle\tau_1\rangle$ increases with loading for $N>N_2$ because adding molecules blocks target W sites.

E. Summary of analytical results

We can now assemble the concentration dependence of the cage-to-cage rate coefficient, $k_\theta=\kappa\cdot k_1\cdot P_1$. For $N<N_2$ we find that:

$$\begin{aligned}k_\theta &\cong \frac{1}{2}\cdot 6\left[k_{1\to1}+\left(1-\frac{N-1}{N_2}\right)k_{1\to2}\right]\cdot\frac{1}{1+\dfrac{N_2-N+1}{N_1\varepsilon}}\\ &\cong \frac{3}{2}\left(k_{1\to1}+\frac{N_2-N+1}{N_2}k_{1\to2}\right)\frac{N_2}{N_2-N+1}e^{-\beta(E_1-E_2)}\end{aligned} \tag{3.31}$$

$$= \frac{3}{2}\left(\frac{N_2}{N_2-N+1}\cdot\frac{k_{1\to1}}{k_{1\to2}}+1\right)k_{2\to1} \tag{3.32}$$

$$\xrightarrow{V\to\infty}\ \frac{3}{2}\left(\frac{2}{2-3\theta}\cdot\frac{k_{1\to1}}{k_{1\to2}}+1\right)k_{2\to1}. \tag{3.33}$$

Equation (3.31) results because $K_{\text{eq}}(1\to2)\gg 1$ for $N\leqslant N_2$. In Eq. (3.32) we substitute $k_{2\to1}/k_{1\to2}$ for $e^{-\beta(E_1-E_2)}$, and in Eq. (3.33) we take the thermodynamic limit.

Several remarks can be made about Eqs. (3.31)–(3.33). As discussed above, Eqs. (3.32) and (3.33) give the correct infinite dilution limit, consistent with Eq. (2.5). The singularity in Eq. (3.33) at $\theta=\frac{2}{3}$, foreshadowed in Fig. 7, is a pathological aspect of the leading order approximation for $K_{\mathrm{eq}}(1\rightarrow 2)$ in the very local neighborhood of $\theta=\frac{2}{3}$. The cage-to-cage rate coefficient is proportional to $K_{\mathrm{eq}}(2\rightarrow 1)$, which is why we plot this quantity in Figs. 5 and 7. The apparent activation energy of k_θ is nearly $E_a(2\rightarrow 1)$ when $E_a(1\rightarrow 1)\cong E_a(1\rightarrow 2)$, as is the case in Table I.

Equation (3.33) predicts a weak, monotonic increase of k_θ with $\theta<\frac{2}{3}$ resulting from a balance among different trends. To see this more clearly, we note that the leading order approximation includes two mechanisms of cage-to-cage motion for $\theta<\frac{2}{3}$, namely $\mathrm{S_{II}}\rightarrow\mathrm{W}\rightarrow\mathrm{S_{II}}$ and $\mathrm{S_{II}}\rightarrow\mathrm{W}\rightarrow\mathrm{W}$ jumps. Both mechanisms are enhanced by increasing W site population, P_1, which increases with loading as $1/(2-3\theta)$. However, k_1 decreases with loading for the $\mathrm{S_{II}}\rightarrow\mathrm{W}\rightarrow\mathrm{S_{II}}$ jump as $2-3\theta$, exactly compensating the W population enhancement. Thus the $\mathrm{S_{II}}\rightarrow\mathrm{W}\rightarrow\mathrm{S_{II}}$ mechanism carries no loading dependence in our model, as indicated by the second term in Eqs. (3.32) and (3.33). On the other hand, k_1 is independent of loading for the $\mathrm{S_{II}}\rightarrow\mathrm{W}\rightarrow\mathrm{W}$ process, giving the residual loading dependence of $1/(2-3\theta)$ for that process, and the only loading dependence in k_θ. As a result, if $k_{1\rightarrow 1}/k_{1\rightarrow 2}\ll 1$, our model predicts essentially no concentration dependence for self-diffusion at low to moderate loadings. Alternatively, if $k_{1\rightarrow 1}/k_{1\rightarrow 2}\not\ll 1$, weak concentration dependence is predicted.

An interesting effect is predicted by Eq. (3.33) for loadings just below $\theta=\frac{2}{3}$. At $T=300$ K and $\theta=0.65$, our analytical approximation remains accurate using the data in Table I. In this case $2/(2-3\theta)\cdot(k_{1\rightarrow 1}/k_{1\rightarrow 2})\cong 12.5\gg 1$, so that $k_\theta\cong 3/(2-3\theta)\cdot(k_{1\rightarrow 1}k_{2\rightarrow 1}/k_{1\rightarrow 2})$. The apparent activation energy in this case is given by:

$$\begin{aligned}E_a&=E_a(1\rightarrow 1)+E_a(2\rightarrow 1)-E_a(1\rightarrow 2)\\&=(E^{\ddagger}_{1\rightarrow 1}-E_1)+(E^{\ddagger}_{2\rightarrow 1}-E_2)-(E^{\ddagger}_{1\rightarrow 2}-E_1)\\&=E^{\ddagger}_{1\rightarrow 1}-E_2,\end{aligned}\tag{3.34}$$

where by microscopic reversibility $E^{\ddagger}_{2\rightarrow 1}=E^{\ddagger}_{1\rightarrow 2}$. This shows how blocking $\mathrm{S_{II}}$ sites at moderately high loadings makes the $\mathrm{S_{II}}\rightarrow\mathrm{W}\rightarrow\mathrm{W}$ process so important that the apparent activation energy changes with loading. We have previously predicted[25] this effect for loadings near $\theta=\frac{2}{3}$ by anticipating the effect of guest–guest interactions. Our present results show that this effect also arises from site blocking in the absence of intracage guest–guest interactions.

The concentration dependence of $k_\theta=\kappa\cdot k_1\cdot P_1$ for $N>N_2$ is given by:

$$k_\theta\cong\frac{1}{2}\cdot 6\left(1-\frac{N-N_2-1}{N_1-1}\right)k_{1\rightarrow 1}\cdot\frac{1}{1+\dfrac{N_2}{N-N_2}}$$

$$=3\left(\frac{N_1+N_2-N}{N_1-1}\right)\left(\frac{N-N_2}{N}\right)k_{1\rightarrow 1}\tag{3.35}$$

$$\xrightarrow{V\rightarrow\infty}3(1-\theta)\left(\frac{3\theta-2}{\theta}\right)k_{1\rightarrow 1}.\tag{3.36}$$

Equations (3.35) and (3.36) predict the correct full loading limit, i.e. $k_\theta=0$ for $\theta=1$, and give a new apparent activation energy for high loadings, namely $E_a=E_a(1\rightarrow 1)$. As a result, the site blocking model predicts that diffusion is faster for $\theta>\frac{2}{3}$ than it is for $\theta<\frac{2}{3}$ by a factor roughly equal to $e^{-\beta(E_2-E_1)}$, since at high loadings molecules are forced to occupy higher energy W sites. Equations (3.35) and (3.36) predict an initial increase in k_θ for $\theta\gtrsim\frac{2}{3}$, resulting from enhanced W population. At higher loadings k_θ reaches a maximum, then decreases as k_1 decreases due to blocking target W sites. Equation (3.36) indicates that diffusion is fastest at $\theta\cong 0.82$, corresponding approximately to four $\mathrm{S_{II}}$ sites and one W occupied per supercage.

In Paper II we report the results of kinetic Monte Carlo simulations on benzene in Na-Y within the site blocking model to test the accuracy of the analytical formulas derived above. We also compare our theory and simulation results against available experimental data. It is shown in Paper II that our analytical formulas agree quantitatively with simulation results, and agree qualitatively with experiment for low to moderate loadings.

IV. CONCLUDING REMARKS

We have developed an analytical expression for the diffusion coefficient of benzene in Na-Y at finite loadings in terms of fundamental rate coefficients. Our theory assumes that a collection of benzene molecules jump among $\mathrm{S_{II}}$ and W binding sites, located near $\mathrm{Na^+}$ ions in 6-rings and in 12-ring windows, respectively. Our diffusion theory is based on a mean field approximation which assumes that instantaneous benzene occupancies in different Na-Y supercages are identical. This yields $D_\theta=\frac{1}{6}k_\theta a_\theta^2$ where $a_\theta\cong 11$ Å is the mean intercage jump length and $1/k_\theta$ is the mean supercage residence time.

We have shown that k_θ is given by $\kappa\cdot k_1\cdot P_1$, where P_1 is the probability of occupying a W site, k_1 is the total rate of leaving a W site, and κ is the probability of cage-to-cage motion when starting from a W site. To be consistent with our earlier mean field approximation, we assume $\kappa=\frac{1}{2}$ for all loadings. Analytical formulas for the temperature and loading dependencies of k_1 and P_1 have been derived assuming that $\mathrm{S_{II}}$ and W site occupancies are either 0 or 1, and that benzenes do not otherwise interact. This site blocking model gives qualitatively accurate results when binding sites are only moderately perturbed by medium to long range guest–guest interactions. The simplicity of the site blocking model allows us to develop exact expressions for P_1 in the canonical and grand canonical ensembles, which are related for finite systems with a new ensemble correspondence rule. For $\theta<\frac{2}{3}$, the $\mathrm{S_{II}}\rightarrow\mathrm{W}\rightarrow\mathrm{S_{II}}$ cage-to-cage jump contributes no loading dependence to k_θ, while the $\mathrm{S_{II}}\rightarrow\mathrm{W}\rightarrow\mathrm{W}$ process gives a monotonically increasing loading dependence of $1/(2-3\theta)$. For $\theta>\frac{2}{3}$, k_θ initially increases due to enhanced W population, then decreases as k_1 decreases due to blocking target W sites. The site blocking model predicts that diffusion is fastest at $\theta\cong 0.82$, corresponding approximately to four $\mathrm{S_{II}}$ sites and one W occupied per supercage. It is shown in Paper II that our analytical formulas agree quantitatively with simulation results, and agree qualitatively with experiment for low to moderate loadings.

Since analytical theories can often display the physics essential to a process more clearly than simulations, and are certainly more desirable in terms of computational effort, it is important to extend the results presented herein to include the effects of medium to long range guest−guest interactions. We will address the importance of these interactions in a forthcoming publication[40] by considering how nearest neighbor S_{II} and W site occupancies affect binding site stabilities and residence times.

Further study is required to determine how widely applicable the approach presented above is to transport problems in other host−guest systems, such as modeling diffusion of other guests, modeling diffusion in silicalite[56] or modeling single file diffusion in channel zeolites.[48–50] Regarding other guest species, our present approach is useful when guests diffuse through zeolites by making infrequent, uncorrelated jumps among relatively deep sorption sites. Regarding diffusion in silicalite, channel intersections are analogous to FAU supercages, while channels are analogous to W sites connecting adjacent supercages. As such, our approach should be applicable to studying mobility in MFI type zeolites. On the other hand, single file diffusion in one dimensional channel zeolites arises because of strong correlations among the relative positions of guest molecules, a phenomenon beyond the scope of our present mean field approximation. Further theoretical advances are required to adapt our present approach to modeling single file diffusion.

ACKNOWLEDGMENTS

The authors thank Dr. Fabien Jousse for many stimulating discussions. S.M.A. acknowledges support from the NSF under grants CHE-9625735 and CHE-9616019, and from Molecular Simulations, Inc. for generously providing visualization software. Acknowledgment is made to the donors of the Petroleum Research Fund, administered by the American Chemical Society, for partial support of this research under grant ACS-PRF 30853-G5.

[1] J. Kärger and D. M. Ruthven, *Diffusion in Zeolites and Other Microporous Solids* (Wiley, New York, 1992).

[2] N. Y. Chen, T. F. Degnan, Jr., and C. M. Smith, *Molecular Transport and Reaction in Zeolites* (VCH, New York, 1994).

[3] Weitkamp J, in *Catalysis and Adsorption by Zeolites*, edited by G. Olhmann, J. C. Vedrine, and P. A. Jacobs (Elsevier, Amsterdam, 1991).

[4] J. M. Newsam, *Zeolites*, in *Solid State Chemistry: Compounds*, edited by A. K. Cheetham and P. Day (Oxford University Press, Oxford, 1992), pp. 234–280.

[5] P. Demontis, S. Yashonath, and M. L. Klein, J. Phys. Chem. **93**, 5016 (1989).

[6] C. R. A. Catlow, C. M. Freeman, B. Vessal, S. M. Tomlinson, and M. Leslie, J. Chem. Soc. Faraday Trans. **87**, 1947 (1991).

[7] R. L. June, A. T. Bell, and D. N. Theodorou, J. Phys. Chem. **95**, 8866 (1991).

[8] M. W. Deem, J. M. Newsam, and J. A. Creighton, J. Am. Chem. Soc. **114**, 7198 (1992).

[9] C. R. A. Catlow, *Modeling of Structure and Reactivity in Zeolites* (Academic, London, 1992).

[10] S. Yashonath and P. Santikary, J. Phys. Chem. **97**, 3849 (1993).

[11] L. M. Bull, N. J. Henson, A. K. Cheetham, J. M. Newsam, and S. J. Heyes, J. Phys. Chem. **97**, 11 776 (1993).

[12] P. R. van Tassel, S. A. Somers, H. T. Davis, and A. V. McCormick, Chem. Eng. Sci. **49**, 2979 (1994).

[13] A. K. Jameson, C. J. Jameson, and R. E. Gerald, J. Chem. Phys. **101**, 1775 (1994).

[14] S. M. Auerbach, N. J. Henson, A. K. Cheetham, and H. I. Metiu, J. Phys. Chem. **99**, 10 600 (1995).

[15] D. Keffer, A. V. McCormick, and H. T. Davis, J. Phys. Chem. **100**, 967 (1996).

[16] H. Klein, H. Fuess, and G. Schrimpf, J. Phys. Chem. **100**, 11 101 (1996).

[17] T. Mosell, G. Schrimpf, C. Hahn, and J. Brickmann, J. Phys. Chem. **100**, 4571 (1996).

[18] F. Jousse, L. Leherty, and D. P. Vercauteren, J. Phys. Chem. B **101**, 4717 (1997).

[19] W. R. Qureshi and J. Wei, J. Catal. **126**, 126 (1990).

[20] J. R. Xiao and J. Wei, Chem. Eng. Sci. **47**, 1123 (1992).

[21] P. Duczynski, Z. Chvoj, V. Chab, M. Ondrejcek, and H. Conrad, Surf. Sci. **331**, 249 (1995).

[22] Z. Chvoj, H. Conrad, and V. Chab, Surf. Sci. **352**, 983 (1996).

[23] G. Czarnecki, M. R. Dudek, A. Pekalski, and J. Cislo, J. Phys. A **29**, 3367 (1996).

[24] J. J. M. Beenakker and I. Kuscer, Zeolites **17**, 346 (1996).

[25] S. M. Auerbach, J. Chem. Phys. **106**, 7810 (1997).

[26] K. A. Fichthorn and W. H. Weinberg, J. Chem. Phys. **95**, 1090 (1991).

[27] D. Barthomeuf and B. H. Ha, J. Chem. Soc. Faraday Trans. **69**, 2158 (1973).

[28] A. N. Fitch, H. Jobic, and A. Renouprez, J. Phys. Chem. **90**, 1311 (1986).

[29] L. Uytterhöven, D. Dompas, and W. J. Mortier, J. Chem. Soc. Faraday Trans. **88**, 2753 (1992).

[30] H. Klein, C. Kirschhock, and H. Fuess, J. Phys. Chem. **98**, 12345 (1994).

[31] P. J. O'Malley and C. J. Braithwaite, Zeolites **15**, 198 (1995).

[32] S. M. Auerbach and H. I. Metiu, J. Chem. Phys. **105**, 3753 (1996).

[33] S. M. Auerbach, L. M. Bull, N. J. Henson, H. I. Metiu, and A. K. Cheetham, J. Phys. Chem. **100**, 5923 (1996).

[34] S. M. Auerbach and H. I. Metiu, J. Chem. Phys. **106**, 2893 (1997).

[35] J. Kärger and D. M. Ruthven, J. Chem. Soc. Faraday Trans. I **77**, 1485 (1981).

[36] M. Bülow, W. Mietk, P. Struve, and P. Lorenz, J. Chem. Soc. Faraday Trans. I **79**, 2457 (1983).

[37] A. Germanus, J. Kärger, H. Pfeifer, N. N. Samulevic, and S. P. Zdanov, Zeolites **5**, 91 (1985).

[38] D. M. Shen and L. V. C. Rees, Zeolites **11**, 666 (1991).

[39] S. Brandani, Z. Xu, and D. Ruthven, Microporous Mater. **7**, 323 (1996).

[40] C. Saravanan and S. M. Auerbach (in preparation).

[41] R. Gomer, Rep. Prog. Phys. **53**, 917 (1990).

[42] D. A. Dougherty, Science **271**, 163 (1996).

[43] M. Wilhelm, A. Firouzi, D. E. Favre, L. M. Bull, D. J. Schaefer, and B. F. Chmelka, J. Am. Chem. Soc. **117**, 2923 (1995).

[44] D. J. Schaefer, D. E. Favre, M. Wilhelm, S. Weigel, and B. F. Chmelka, J. Am. Chem. Soc. (in press).

[45] D. Chandler, *Introduction to Modern Statistical Mechanics* (Oxford University Press, New York, 1987).

[46] D. Stauffer and A. Aharony, *Introduction to Percolation Theory* (Taylor and Francis, Bristol, 1991).

[47] A. W. Adamson, *Physical Chemistry of Surfaces*, 5th ed. (Wiley, New York, 1990).

[48] V. Kukla, J. Kornatowski, D. Demuth, and I. Gimus, Science **272**, 702 (1996).

[49] K. Hahn, J. Kärger, and V. Kukla, Phys. Rev. Lett. **76**, 2762 (1996).

[50] D. Keffer, A. V. McCormick, and H. T. Davis, Mol. Phys. **87**, 367 (1996).

[51] C. Saravanan and S. M. Auerbach (submitted).

[52] R. C. Tolman, *The Principles of Statistical Mechanics* (Oxford University Press, New York, 1938).

[53] N. J. Henson, Ph.D. thesis, Oxford University, 1996.

[54] G. Arfken, *Mathematical Methods for Physicists* (Academic, San Diego, 1985).

[55] M. F. Allen and D. J. Tildesley, *Computer Simulation of Liquids* (Oxford Science, Oxford, 1987).

[56] R. Q. Snurr, A. T. Bell, and D. N. Theodorou, J. Phys. Chem. **98**, 11 948 (1994).